Pergamon

SCIENCE DIRECT®

Tetrahedron 59 (2003) 10059–10073

TETRAHEDRON

Fluorinated photosensitizers: synthesis, photophysical, electrochemical, intracellular localization, in vitro photosensitizing efficacy and determination of tumor-uptake by ^{19}F in vivo NMR spectroscopy

Suresh K. Pandey,[a] Amy L. Gryshuk,[a] Andrew Graham,[b] Kei Ohkubo,[c] Shunichi Fukuzumi,[c,*] Mahabeer P. Dobhal,[a,†] Gang Zheng,[a] Zhongping Ou,[d] Riqiang Zhan,[d] Karl M. Kadish,[d,*] Allan Oseroff,[b] S. Ramaprasad[e,*] and Ravindra K. Pandey[a,f,*]

[a]*Photodynamic Therapy Center, Roswell Park Cancer Institute, Elm and Carlton Streets, Buffalo, NY 14263, USA*
[b]*Department of Dermatology, Roswell Park Cancer Institute, Buffalo, NY 14263, USA*
[c]*Department of Material and Life Science, Graduate School of Engineering, Osaka University, CREST, Japan Science and Technology Agency (JST), Yamada-oka, Suita, Osaka 565-0871, Japan*
[d]*Department of Chemistry, University of Houston, Houston, TX 77204-5003, USA*
[e]*Department of Radiology, University of Nebraska, Omaha, Nebraska, USA*
[f]*Department of Nuclear Medicine, Roswell Park Cancer Institute, Buffalo, NY 14263, USA*

Received 4 September 2003; revised 6 October 2003; accepted 6 October 2003

Abstract—For in vivo NMR studies, starting from pyrroles, a series of fluorinated porphyrins were synthesized by following the MacDonald reaction conditions. Upon reaction with osmium tetroxide, a fluorinated porphyrin containing four trifluoromethyl groups (12 fluorine units) was converted into the related chlorin and bacteriochlorin which exhibited long-wavelength absorptions at 652 and 720 nm, respectively. All compounds produced good singlet oxygen production efficiency. A comparative study of nine porphyrins with and without fluorine substituents indicated no adverse effects of the presence of fluorinated groups in the photophysical properties of the porphyrins, chlorins or bacteriochlorins. The first and second one-electron reduction potentials (vs SCE) of the investigated compounds range between −1.29 and −1.49 V and between −1.66 and −1.84 V in PhCN containing 0.1 M TBAP. UV–visible spectroelectrochemical data suggested the formation of π-anion and π-cation radicals upon the first reduction and first oxidation. The in vivo ^{19}F MR study of a representative fluorine labeled compound with twelve equivalent fluorines confirmed the presence of the fluorine labeled sensitizer in mouse (C3H/HeJ) implanted with RIF tumors on mouse foot dorsum by inoculating 2×10^5 cells (the studies were repeated on four tumored mice to confirm the feasibility and reproducibility). All fluorinated compounds were found to be quite effective in vitro. In a comparative intracellular localization study with Rhodamine-123 in RIF tumor cells, the most soluble porphyrin containing two propionic ester side chains was found to localize in mitochondria as well as the related chlorin and bacteriochlorin.

1. Introduction

Photodynamic therapy (PDT) is now a well recognized modality that has been used both independently and in conjunction with other cancer treatments.[1] Combining the use of a light-sensitive drug, lasers and fiber-optic probes, PDT has emerged as one of the promising strategies in cancer treatment. In this therapy, patients are given intravenous injections of a drug that accumulates in cancer cells in much higher concentrations than in normal cells. Laser light with an appropriate wavelength delivered by fiber optics to these tumor sites produces highly reactive oxygen species (e.g. $^1O_2$) that destroy the tumor cells.[2] Therefore, for a drug to be effective, it is necessary that the compound be in high concentration in tumor cells. PDT is most beneficial when laser light is delivered at a time point when the photosensitizer's concentration is greater in the tumor than in the surrounding tissue. Thus, a comprehensive knowledge of the extent of localization and the rate of accumulation is of immense value. While the photo sensitizer's concentration in tissue may be determined by chemical extraction techniques, these methods are

Keywords: photodynamic therapy; photosensitizers; porphyrins; chlorins; bacteriochlorins; mitochondria.
* Corresponding authors. Address: Photodynamic Therapy Center, Roswell Park Cancer Institute, Elm and Carlton Streets, Buffalo, NY 14263, USA. Tel.: +1-7168453203; fax: +1-7168458920;
e-mail: ravindra.pandey@roswellpark.org;
fukuzumi@ap.chem.eng.osaka-u.ac.jp; kkadish@uh.edu;
sramaprasad@unmc.edu
† On leave from the Department of Chemistry, University of Rajasthan, Jaipur 302004, India.

0040–4020/$ - see front matter © 2003 Elsevier Ltd. All rights reserved.
doi:10.1016/j.tet.2003.10.016

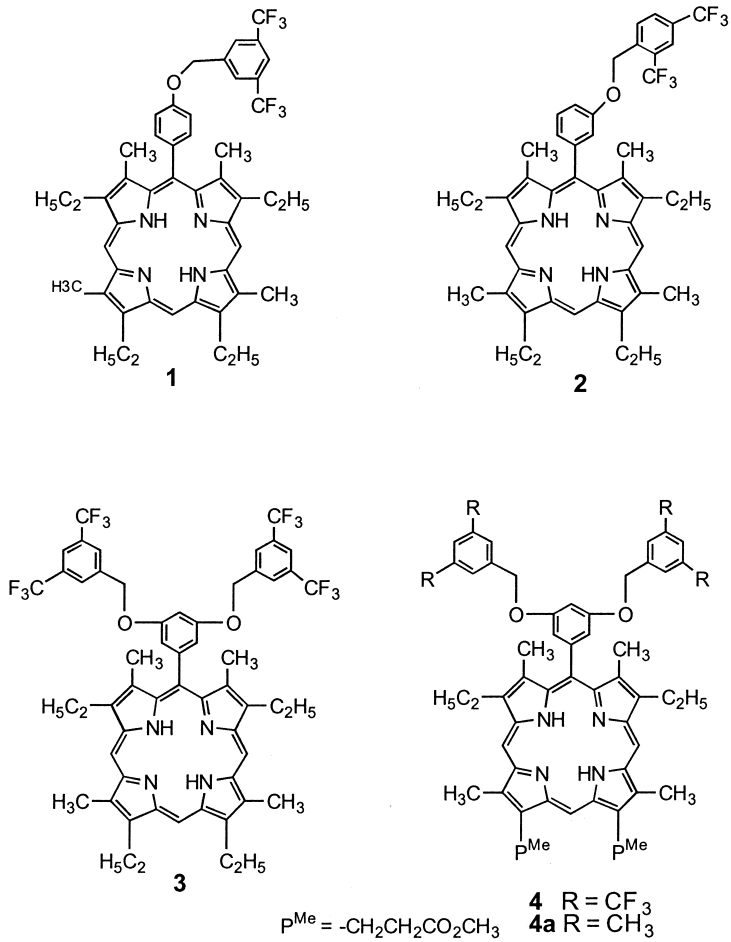

Chart 1.

invasive, time consuming, and clinically non-feasible. In contrast, in vivo NMR is minimally invasive, considered safe, and the therapy can be monitored over time in a single living system.[3]

In vivo MR spectroscopy has been used increasingly to monitor metabolism and disease states in humans. Both magnetic resonance imaging and spectroscopy have evolved into sophisticated diagnostic techniques. In addition to the proton, nuclei such as fluorine[4] can be studied by in vivo spectroscopy and imaging. Fluorine-19 (^{19}F) NMR is a technique with significant potential because of the relatively high sensitivity and low endogenous background. Due in part to its high MR sensitivity, fluorine has received considerable attention as an MR nucleus. Fluorine-19 MR has been used to study metabolism, tumor growth, and blood flow.[5] More recently, in vivo ^{19}F MR has been used to measure tumor integrity and vasculature in subcutaneously implanted tumors in rats.[6] MR of fluorinated compounds is particularly attractive for in vivo studies of human and animal models. The ^{19}F isotope has a 100% natural abundance, a spin of 1/2, and a MR sensitivity that is 83% then that of hydrogen.[7]

To date, most of the fluorinated porphyrin-based analogs synthesized for in vivo ^{19}F NMR studies have been unsymmetrical,[8] and thus lead to signal dispersion. In order to have a strong fluorine signal at a low concentration of the drug in tumors, it is necessary to have photosensitizers containing multiple fluorine units. It would be advantageous to have a photosensitizer with equivalent fluorine substituents that will render signal addition of all equivalent nuclei.

In this manuscript we report the synthesis of a series of fluorinated and the corresponding non-fluorinated porphyrin-based compounds, the effect of the substituents on their photophysical and electrochemical characteristics, their intracellular localization and their in vitro photosensitizing efficacy.

2. Results and discussion

2.1. Chemistry

For the synthesis of porphyrin-based fluorinated photosensitizers, our synthetic strategy was divided into two parts. These were the (a) synthesis of porphyrins **1** and **2** containing symmetrical trifluoromethyl groups (total fluorine: 6) introduced at the *meta*-or *para*-position(s) of the phenyl ring and (b) porphyrins **3** and **4** bearing symmetrical trifluoromethyl groups introduced at the 3 and 5-positions (total fluorine: 12) of the phenyl ring present at the *meso*-position of the porphyrin ring system (see Chart 1).

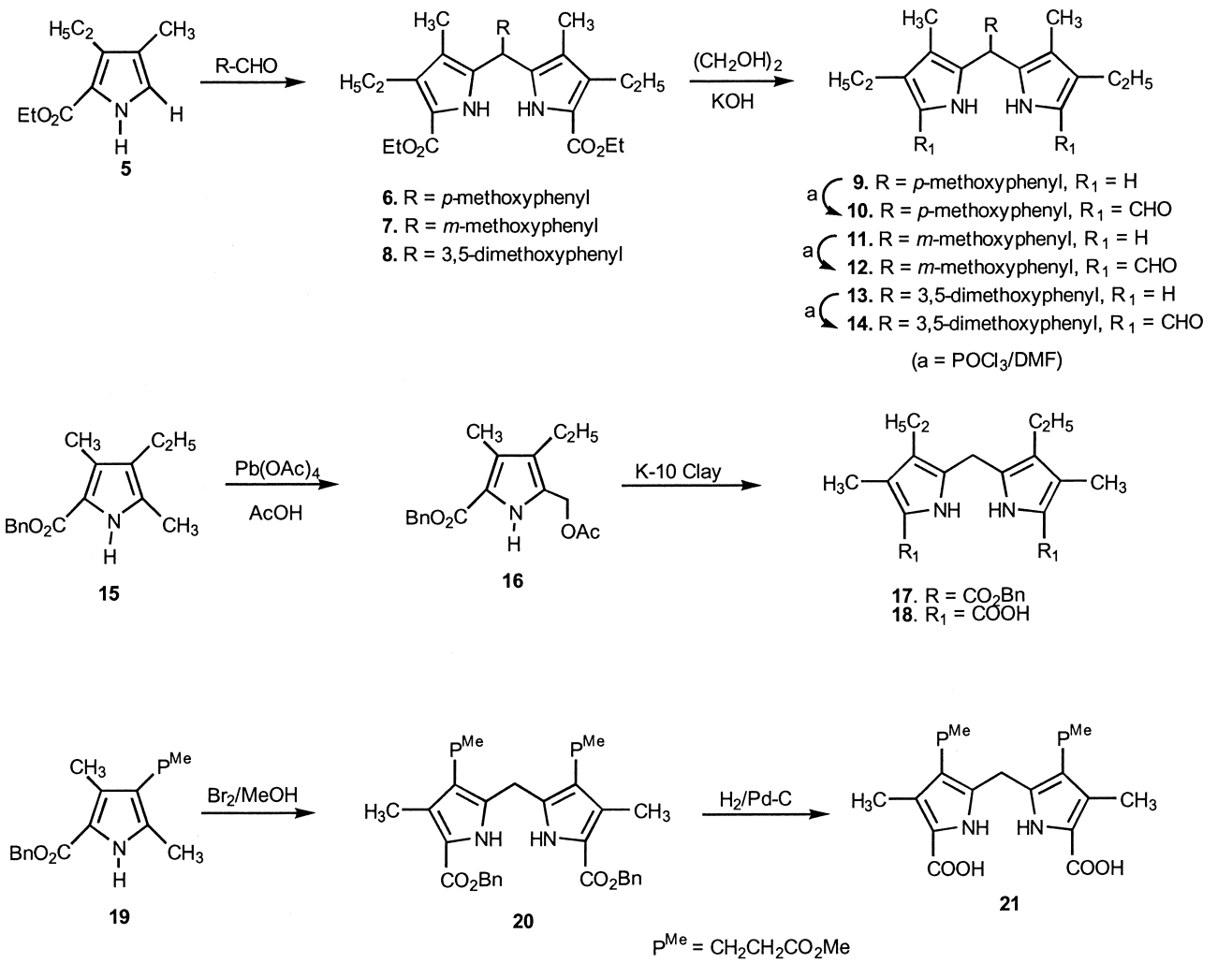

Scheme 1.

Porphyrins **1**–**4** were synthesized from pyrroles **5**,[9] **15**[10] or **19**[11] by following the well established '2+2' reaction approach[12] (see Scheme 1). In brief, reactions of pyrrole **5** with *p*-, *m*- or 3′,5′-dimethoxyphenyl aldehyde under acidic reaction conditions produced the corresponding dipyrromethanes **6**, **7** and **8** in 60–80% yield, which on refluxing with ethylene glycol/KOH gave the related α-free dipyrromethanes **9**, **11** and **13**, respectively in >85% yield. Further reaction of these dipyrromethanes with $POCl_3$/DMF under Vilsmeier's reaction conditions[13] produced the corresponding diformyl dipyrromethanes **10**, **12** and **14** in excellent yields (>75%). For the preparation of dipyrromethane **17**, pyrrole **15** was first converted into the acetoxy derivative **16**, which on treating with K-10 clay[14] in dichloromethane at room temperature gave the desired dipyrromethane in 70% overall yield. Reaction of pyrrole **19** with bromine/methanol[15] gave the corresponding dipyrromethane **20** in 72% yield. Hydrogenation of dipyrromethane **17** and **20** in presence of Pd/C at room temperature produced the corresponding carboxylic acids **18** and **21** in quantitative yields.

Diformyldipyrromethanes **10**, **12** and **14** were then individually reacted with dipyrromethane dicarboxylic acid **18** under McDonald reaction conditions.[12] After purification porphyrins **22**–**24** were isolated in modest yield. By following a similar approach, pyrromethane **14** was also reacted with pyrromethane dicarboxylic acid **21**, and porphyrin **25** was obtained in 38% yield. For the preparation of the fluorinated analogs, porphyrins **22**–**25** containing methoxy groups in the phenyl rings were reacted with boron tribromide and the related hydroxyphenyl porphyrins **26**–**29** were obtained in 70–77% yields. Further reaction of these porphyrins with 3,5-trifluoromethylbenzyl bromide produced the desired fluorinated porphyrins **1**–**4** in modest yield (Scheme 2). Reaction of **29** with 3,5-dimethylbenzyl bromide produced the non-fluorinated porphyrin **4a** in good yield. The structures of the intermediates and the final products were confirmed by ^1H, ^{19}F NMR, mass spectrometry and elemental analyses.

Among the fluorinated porphyrins **1**–**4**, compound **4**, containing two propionic ester functionalities at the bottom half of the molecule showed enhanced solubility compared to those containing alkyl groups in 1% Tween 80/water formulation as well as improved in vitro photosensitizing efficacy in comparison to the other analogues. Therefore, for investigating the photosensitizing effect(s) of fluorinated groups in long-wavelength absorbing compounds, porphyrin **4** was reacted with osmium tetroxide (OsO_4) and

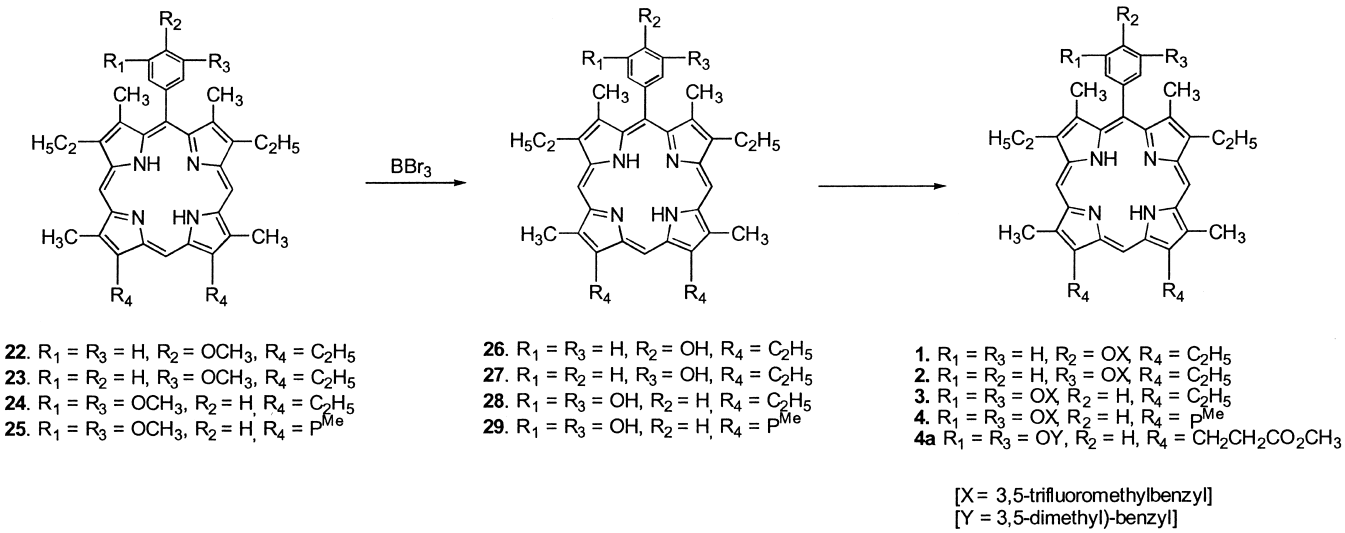

Scheme 2.

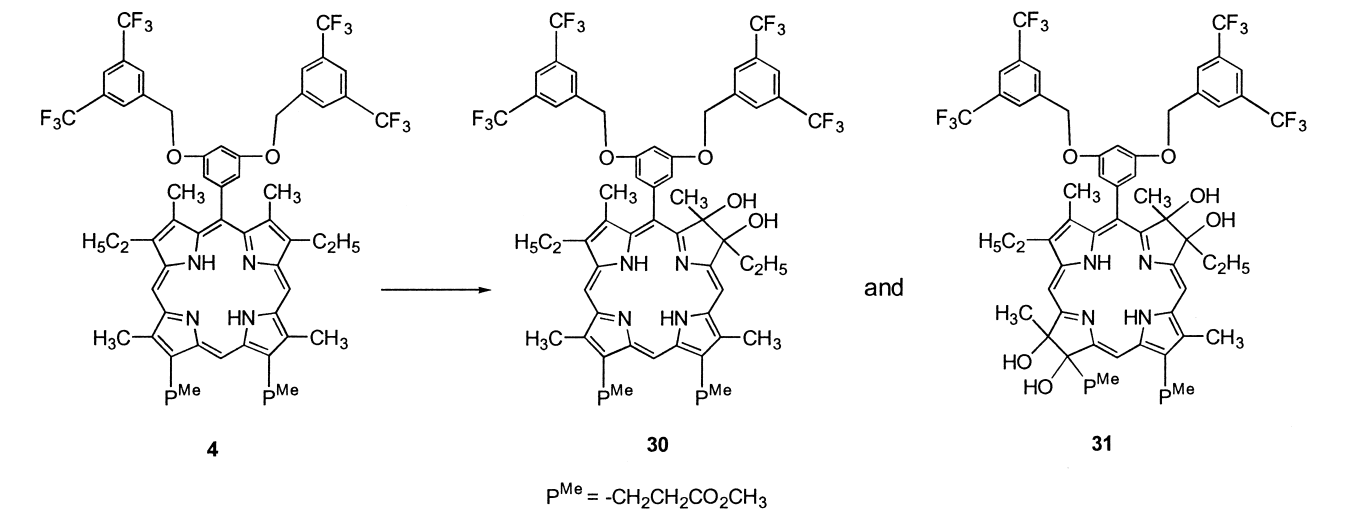

Scheme 3.

the corresponding *vic*-dihydroxy chlorin **30** (λ_{max}: 648 nm) and tetra-hydroxy-bacteriochlorin **31** (as an isomeric mixture, λ_{max}: 716 nm) were synthesized. The relative yields of **31** and **32** were found to depend on the amount of OsO_4 used (Scheme 3).

As expected, the ^{19}F NMR spectra of all the fluorinated porphyrins **1**–**4** exhibited a single peak at δ 13.0 ppm, whereas chlorin **30** and bacteriochlorin **31** showed two peaks with equal intensity at 12.98 and 12.99 ppm, respectively.

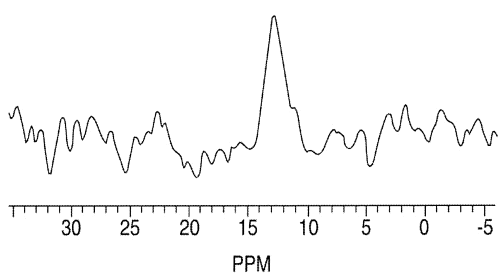

Figure 1. In vivo F-19 NMR spectrum of compound **4** obtained from a RIF tumor implanted in a C3H/HeJ mouse foot dorsum in one of the hind legs.

2.2. In vivo ^{19}F MR spectral characteristics

A typical ^{19}F MR spectrum of the fluorinated photosensitizer recorded on a 7T animal imager 8.0 h post IP administration of the compound (100 $\mu M\ kg^{-1}$) is shown in Figure 1. The tumor volume was 0.18 mL and spectra were recorded over 30 min. The ability to observe the photosensitizer by ^{19}F MR non-invasively is an important step towards understanding its pharmacokinetic characteristics and relating these to its in vivo photosensitizing efficacy. These details will be published elsewhere.

2.3. Photophysical properties

A typical fluorescence spectrum of fluorinated porphyrins in PhCN is shown in Figure 2. For the case of **3**, virtually the same fluorescence maxima at 628 and 693 nm was observed as for non-fluorinated porphyrins. The absorption and fluorescence maxima of investigated porphyrins **1**–**4**,

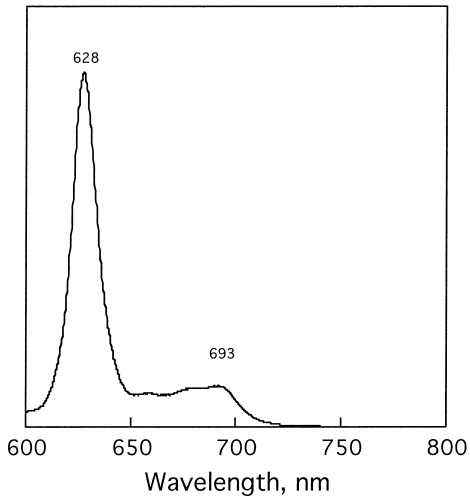

Figure 2. Fluorescence spectrum of **3** (7.3×10^{-6} M) in deaerated PhCN at 298 K by excitation at 535 nm.

26–**29**, chlorin **30** and bacteriochlorin **31** are listed in Table 1. The absorption and the fluorescence maxima are red-shifted in the order: porphyrin, chlorin and bacteriochlorin, but they are not affected by the fluorine substituents.

The fluorescence decay of **3** is well fitted by a single exponential line with lifetime of 18.5 ns as shown in Figure 3. The fluorescence lifetimes are also listed in Table 1. The fluorescence lifetimes (τ) are also unaffected by fluorinated substituents. The τ values of the nine porphyrins in this table are all similar in the range of 16.1–18.6 ns irrespective of substituents, but they are significantly longer than those of chlorin **30** (3.8 ns) and bacteriochlorin **31** (3.3 ns).

Phosphorescence spectra were observed in deaerated frozen 2-MeTHF at 77 K. The phosphorescence maxima are also summarized in Table 1. Again the phosphorescence maxima of porphyrins (822–823 nm) are not affected by the fluorinated substituents. The triplet excited states of the porphyrins were detected from the transient absorption spectra measured 4.0 ns after laser excitation at 355 nm. A typical example is shown in Figure 4 for the case of **3**. The negative absorption at 410 nm in Figure 3 is due to bleaching of the ground-state absorption bands. The positive absorption at 450 nm in Figure 4 is due to the triplet–triplet (T–T) transition. The T–T absorption decay obeys first-order kinetics as shown in Figure 5. This indicates that there is no contribution of the triplet–triplet annihilation under the present experimental conditions.

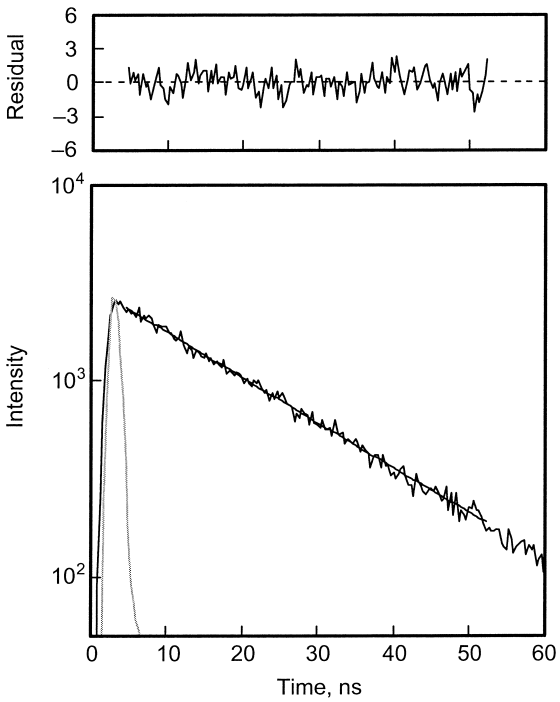

Figure 3. Fluorescence decay (λ_{em}=628 nm) of **3** (7.3×10^{-6} M) in deaerated PhCN at 298 K by excitation at 535 nm. The instrument response (gray line), decay data (solid line), and single-exponential fitted line are plotted in the bottom frame. The residuals of the fit for a lifetime of τ=18.5 ns are plotted in the top frame.

The T–T absorption maxima and the triplet lifetimes are summarized in Table 2. The triplet lifetimes of porphyrins are in the range of 8.3–25 μs, which are shorter than the lifetimes of chlorin **30** (185 μs) and the bacteriochlorin **31** (77 μs).

The decay of the T–T absorption in oxygen-saturated PhCN is enhanced significantly over that observed in deaerated PhCN. The decay rate obeys first-order kinetics and the decay rate constant increases with increasing oxygen concentration. Thus, an efficient energy transfer from the triplet excited state of **3** to oxygen occurs to produce singlet oxygen. The rate constants of the energy transfer (k_{EN}) were

Table 1. Fluorescence emission maxima and fluorescence lifetimes in deaerated PhCN at 298 K, and phosphorescence emission maxima in deaerated 2-MeTHF at 77 K

	λ_{max}(fluorescence) (nm)		τ (fluorescence)[a] (nm)	λ_{max}(phosphorescence) (nm)
26	628	693	18.5	822
27	627	693	17.9	822
28	628	693	17.3	822
29	628	692	17.6	823
1	628	693	18.6	823
2	627	692	16.1	823
3	628	693	18.5	822
4	628	691	17.7	822
4a	629	693	18.2	822
30	652	[b]	3.8	842
31	720	[b]	3.3	806

[a] The experimental errors are within ±5%.
[b] Shoulder peak.

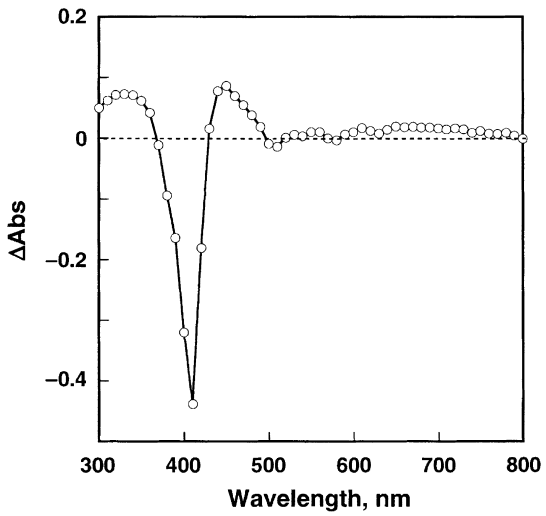

Figure 4. T–T absorption spectrum of **3** (7.3×10^{-6} M) obtained by the laser flash photolysis in deaerated PhCN at 4.0 μs after laser excitation (355 nm) at 298 K.

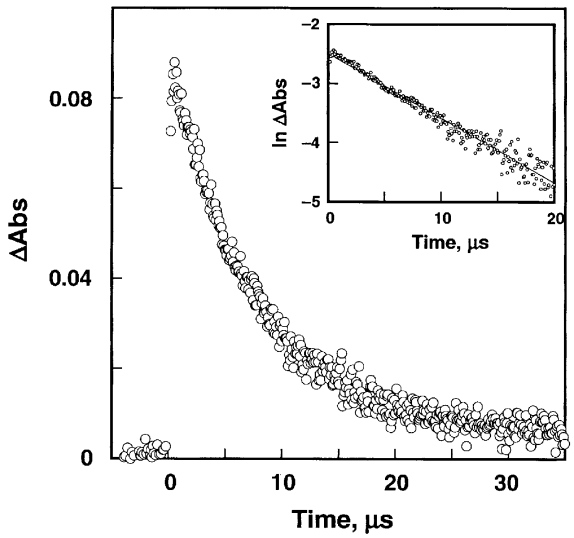

Figure 5. Kinetic trace for the T–T absorption of **3** (7.3×10^{-6} M) at 450 nm in deaerated PhCN after laser excitation (355 nm) at 298 K. Inset: First-order plot.

Table 2. T–T absorption maxima (λ_{max}(T–T)), triplet lifetimes (τ(T–T)) in the deaerated PhCN at 298 K, quenching rate constants of the triplet excited states by oxygen in PhCN, and quantum yields of singlet oxygen in C_6D_6

	λ_{max}(T–T) (nm)	τ(T–T) (s)[a]	k_{EN} (M^{-1} s^{-1})[a]	$\Phi(^1O_2)$[a]
26	450	1.0×10^{-5}	9.4×10^{8}	0.26
27	450	1.1×10^{-5}	1.1×10^{9}	0.57
28	450	1.1×10^{-5}	1.0×10^{9}	0.68
29	450	1.1×10^{-5}	8.9×10^{8}	0.33
1	450	8.3×10^{-6}	9.9×10^{8}	0.61
2	450	1.4×10^{-5}	9.0×10^{8}	0.75
3	450	1.9×10^{-5}	1.0×10^{9}	0.81
4	450	2.5×10^{-5}	1.0×10^{9}	0.36
4a	450	2.3×10^{-5}	9.7×10^{8}	0.27
30	440	1.9×10^{-4}	1.1×10^{9}	0.30
31	440	7.7×10^{-5}	1.1×10^{9}	0.31

[a] The experimental errors are within ±5%.

determined from the dependence of the decay rate constants on oxygen concentration as listed in Table 2. The k_{EN} values are in the range of 8.9×10^{8}–1.1×10^{9} M^{-1} s^{-1}. There is no specific effects of the fluorinated substituents on the k_{EN} values which are smaller than the diffusion-limited value in PhCN (5.6×10^{9} M^{-1} s^{-1}).[16]

Irradiation of an oxygen-saturated benzene solution of **3** results in formation of singlet oxygen which was detected by the $^1O_2$ emission at 1270 nm (see Section 3). Quantum yields (Φ) of $^1O_2$ generation were determined from the emission intensity which was compared to the intensity obtained using a C_{60} reference compound.[17] Relatively high Φ values are obtained for all investigated compounds as summarized in Table 2. The highest Φ value is obtained as 0.81 for the tetrafluorinated compound **3**.

2.4. Electrochemical studies

The electrochemically investigated compounds can be divided into three groups based on the macrocycle and substitutents. The first group includes the four fluorinated porphyrins **1**, **2**, **3** and **4** (Chart 1, Scheme 2), the second, the four non-fluorinated porphyrins **26**, **27**, **28** and **29** (Scheme 2) and the third, the one fluorinated chlorin **30** and the one fluorinated bacteriochlorin **31** (Scheme 3). The electrochemistry of these ten complexes was carried out in PhCN containing 0.1 M TBAP as supporting electrolyte. The half-wave or peak potential for each reduction is listed in Table 3.

In all but one case (compound **29**), the first reduction was reversible and the second irreversible due to a chemical reaction following formation of the dianion. This led to cyclic voltammograms of the type illustrated in Figure 6. A chemical reaction also followed the first oxidation of each porphyrin and this led to irreversible or quasi-reversible oxidations as graphically shown in Figure 7 for the case of compounds **3** and **4**. The UV–visible spectral changes obtained upon the first reduction were recorded in PhCN containing 0.2 M TBAP. An example of the thin-layer spectral changes are shown in Figure 8 for compounds **3** and **30** and a summary of the spectral data for the eight singly reduced porphyrins is given in Table 3. The neutral compounds have a Soret band at 407–412 nm and four visible bands between 503 and 626 nm (see Table 4). Upon the first reduction, the Soret and visible bands decrease in intensity while a new broad visible band appears at 799–813 nm (see Table 3). These results are consistent with a one-electron addition to the porphyrin π-ring system and indicate the formation of a porphyrin π-anion radical.[18] The cyclic voltammograms illustrating the stepwise oxidation of compounds **3**, **4** and **30** are shown in Figure 7. The same spectral patterns are observed for the eight porphyrins in Table 3 and these data may be contrasted to what is observed for reduction of the chlorin **30** (Fig. 8(b)) and bacteriochlorin **31** whose π-anion radical absorption bands are also summarized in this table. The spectral changes obtained upon oxidation of the porphyrin **3** and the chlorin **30** are illustrated in Figure 8. The reaction of the porphyrin is quasi-reversible while that of the chlorin is reversible on the cyclic voltammetry timescale (see cyclic voltamogram Figure 7). Thus only the spectrum of the chlorin **30**

Table 3. Reduction potentials of investigated complexes and UV–visible spectral data of singly reduced compounds in PhCN containing 0.1 M TBAP

Group	Compound	Potential (V vs. SCE)		Singly reduced complexes			
		$E_{1/2}$	E_p	λ_{max}, nm ($\varepsilon\times10^{-4}$, M^{-1} cm^{-1})			
I	**1**	−1.43	−1.78	409 (6.1)	432 (4.9)[sh]	–	806 (0.7)
	2	−1.38	−1.80	408 (5.7)	435 (3.7)[sh]	–	813 (1.0)
	3	−1.40	−1.80	407 (4.3)	–	–	801 (0.9)
	4	−1.29	−1.66	412 (7.1)	–	–	801 (1.1)
II	**26**	−1.44	−1.68	410 (6.8)	434 (6.3)	–	799 (1.8)
	27	−1.44	−1.62	409 (5.1)	437 (4.1)	–	800 (1.9)
	28	−1.49	−1.66	409 (5.7)	439 (2.8)	–	800 (1.0)
	29	−1.46[a]	−1.66	408 (5.2)	439 (2.5)[sh]	–	800 (1.2)
III	**30**	−1.30	−1.74	402 (3.5)	–	535 (0.7)	735 (1.2)
	31	−1.46[b]	−1.84	406 (6.8)	–	750 (0.8)	827 (0.8)

[a] E_p at a scan rate of 0.1 V/s. Two small peaks at E_p=−0.52 and −0.94 V also can be seen on first scan.
[b] A peak at E_p=−1.29 V also can be seen. sh=shoulder peak.

corresponds to a true measurement of the first electrogenerated oxidation product which should be a π-cation radical. The oxidations of other compounds were not chemically or electrochemically reversible and thus no meaningful spectra could be obtained (Fig. 9).

2.5. In vitro photosensitizing efficacy

The in vitro photosensitizing activity of fluorinated photosensitizers **1**–**4** was determined in radiation induced fibrosarcoma (RIF) tumor cell lines.[19] For determining the drug dose, one of the fluorinated porphyins **4** was initially tested at two different concentrations (0.5 and 1.0 μM). The drug concentration at 1.0 μM, together with a light dose at

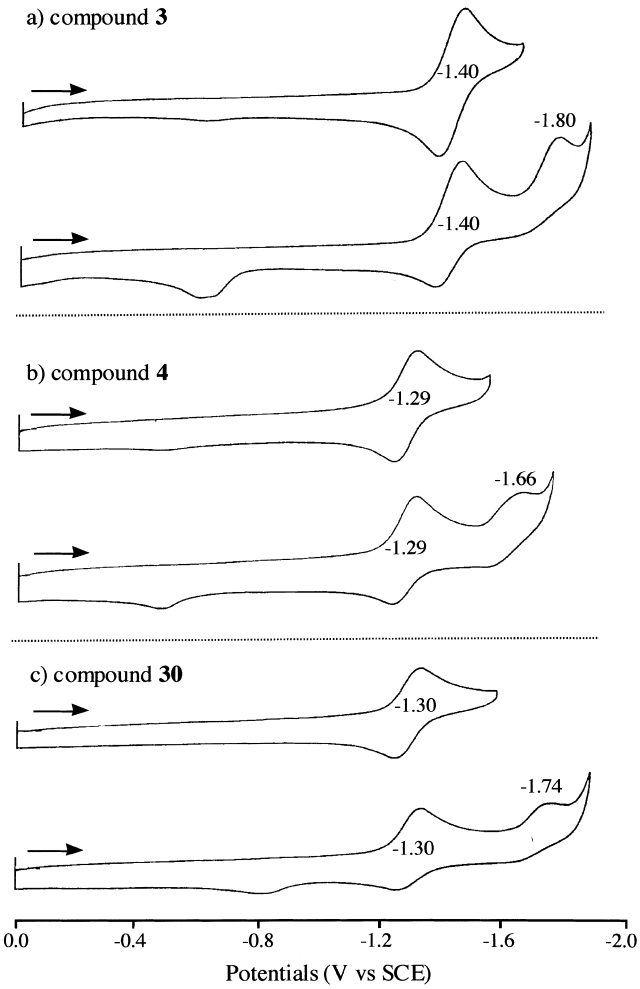

Figure 6. Cyclic voltammograms illustrating the stepwise reductions of compounds (a) **3**, (b) **4** and (c) **30** in PhCN containing 0.1 M TBAP.

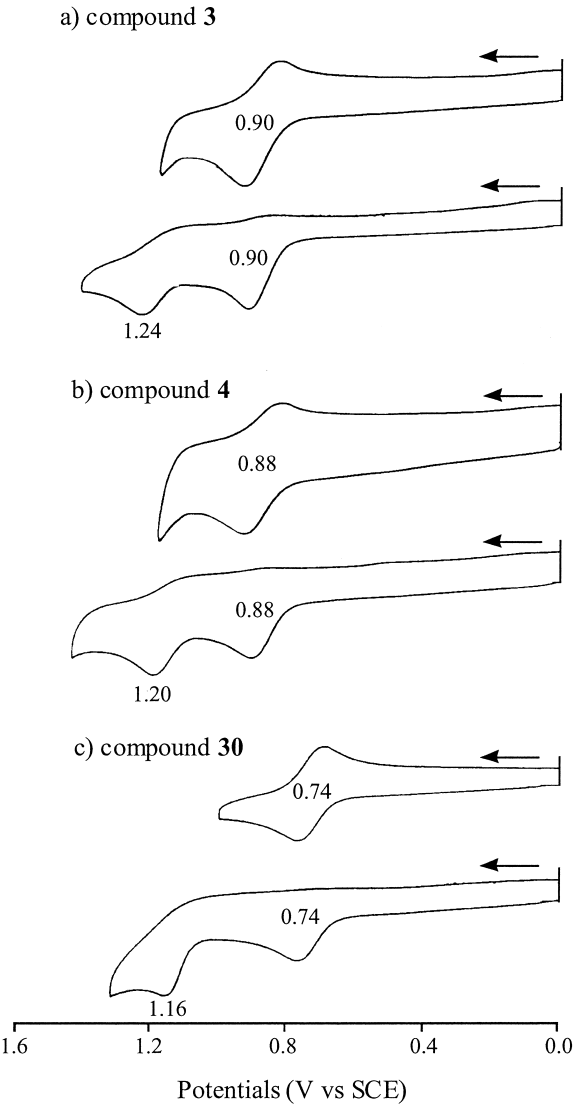

Figure 7. Cyclic voltammograms illustrating the stepwise oxidation of compounds (a) **3**, (b) **4** and (c) **30** in PhCN containing 0.1 M TBAP.

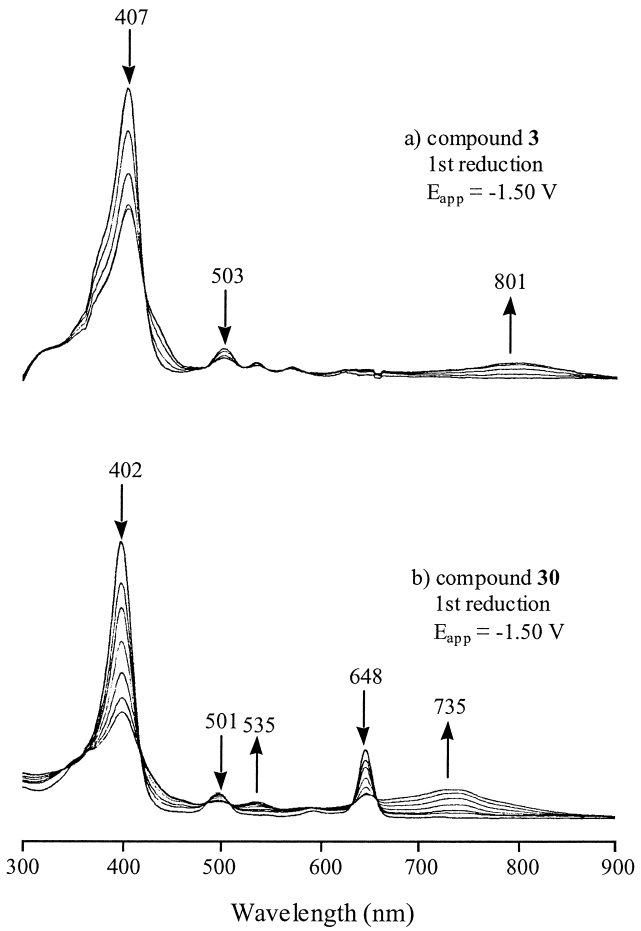

Figure 8. Thin-layer UV–visible spectral changes of (a) compound **3** and (b) compound **30** upon the first reduction at −1.50 V in PhCN containing 0.2 M TBAP.

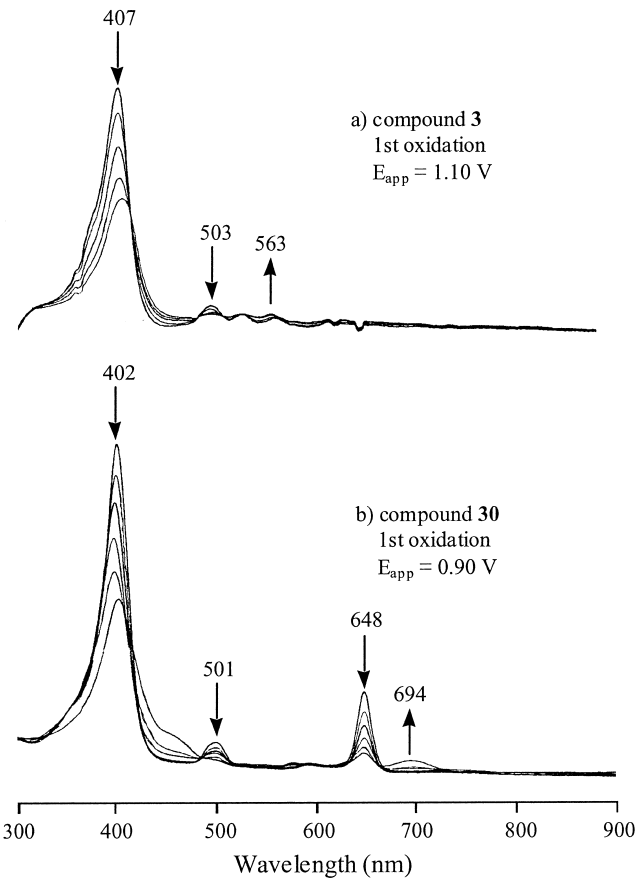

Figure 9. Thin-layer UV–visible spectral changes of (a) compound **3** and (b) compound **30** upon the first oxidation at 1.10 and 0.90 V in PhCN containing 0.2 M TBAP.

4.0 J/cm^2, produced a significant phototoxicity without any dark toxicity. Other photosensitizers were then evaluated under similar drug concentration. From the results summarized in Figure 10 it can be seen that all the fluorinated porphyrins, the chlorin and the bacteriochlorin produced significant in vitro efficacy. However, the compounds in the porphyrin series containing bis-trifluoromethyl groups were found to be less effective than those containing tetrakis-trifluoromethyl groups. The *vic*-dihydroxy chlorin **30** and the related tetrahydroxy bacteriochlorin **31** were quite effective with similar efficacy. In order to correlate the singlet oxygen efficiency with photosensitizing activity, these compounds were also evaluated for their photophysical characteristics. Although the presence and position of the fluorinated substituents in the porphyrin macrocycle produced a remarkable difference in singlet oxygen producing efficiency, no direct correlation was observed between singlet oxygen yield and in vitro photodynamic activity. For example, the singlet oxygen yields of porphyrins **1**–**3**, are quite similar (0.61–0.81) but these compounds showed a significant difference in photosensitizing activity. In contrast, similar photosensitizing results were obtained among the tetrakis-trifluorinated

Table 4. UV–visible data of investigated compounds in PhCN containing 0.2 M TBAP

Group	Compound	λ_{max}, nm ($\varepsilon\times10^{-4}$, M^{-1} cm^{-1})				
		Soret band	Visible bands			
I	**4**	408 (12.71)	503 (1.13)	536 (0.51)	572 (0.47)	626 (0.19)
	2	409 (11.23)	503 (0.74)	538 (0.60)	572 (0.74)	624 (0.29)
	3	407 (7.25)	503 (0.65)	535 (0.30)	571 (0.27)	625 (0.10)
	1	407 (13.12)	503 (1.29)	535 (0.62)	572 (0.58)	625 (0.28)
II	**26**	407 (16.20)	504 (1.24)	536 (0.27)	573 (0.23)	624 (0.09)
	27	407 (12.47)	503 (0.48)	535 (0.20)	572 (0.16)	624 (0.10)
	29	412 (12.70)	504 (0.57)	538 (0.74)	570 (0.95)	615 (0.21)
	28	407 (9.58)	503 (0.88)	535 (0.40)	572 (0.37)	624 (0.15)
III	**30**	402 (8.28)	501 (0.79)	548 (0.17)	593 (0.26)	648 (2.12)
	31	399 (8.90)	506 (1.28)	593 (0.35)	645 (2.02)	715 (1.70)

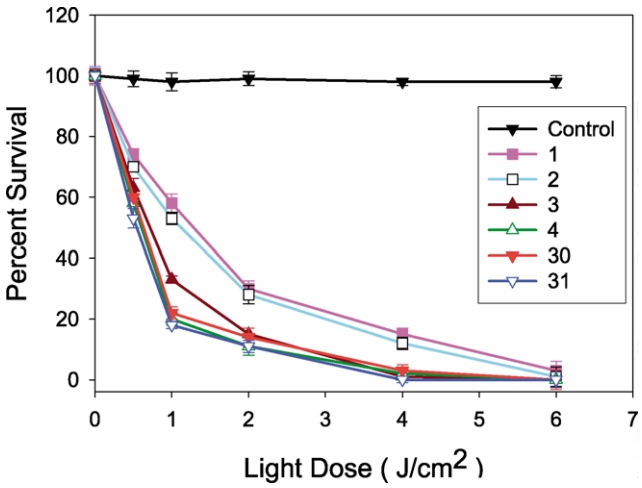

Figure 10. The in vitro photosensitizing activity of various fluorinated porphyrins **1**–**4**, chlorin **30** and bacteriochlorin **31** (1.0 μM) in RIF tumor cells at 4 h incubation. Control: Cell exposed to light without photosensitizer and cells with photosensitizer but no light exposure.

analogs (**3** and **4**) in spite of a significant difference in singlet oxygen yields (0.81 and 0.36, respectively).

On the basis of in vitro results, it is difficult to predict the in vivo photosensitizing efficacy of these photosensitizers because the pharmacokinetic and pharmacodynamic profiles as well as photobleaching characteristics play important roles in drug localization and clearance. These properties could also be influenced by the overall lipophilicity of the molecule which has proven to be an important molecular descriptor that often is well correlated with the bioactivity of drugs. The lipophilicity is indicated by lipophilic indice such as the logarithm of a partition coefficient, log P, which reflects the equilibrium partitioning of a molecule between a non-polar and a polar phase, such as *n*-octanol/water system. Partition coefficients can be measured either experimentally by following a simple 'shake flask' approach or by using a currently available computer program (PALLAS system).[19c] We calculated the log *P* values of the fluorinated porphyrins **1**–**4**, the chlorin **30** and the bacteriochlorin **31** and these were in the range of 12.76–19.75 [**1** and **2**: 15.58, **3**: 19.75, **4**: 18.43, **30**:15.60 and **31**:12.76]. For investigating a correlation between singlet oxygen yields and PDT efficacy, the in vivo studies of fluorinated photosensitizers at different drug/ight doses are currently in progress. These results along with the in vivo ^{19}F tumor imaging data will be reported elsewhere.

2.6. Intracellular localization

In general, porphyrin-based compounds have shown very diverse patterns of localization, based on structure, lipophilicity and charge.[20] Localization in the lysosomes and mitochondria are reported to be predominant. However, in a QSAR study of certain photosensitizers the compounds that localize in mitochondria are generally found to be more effective. Therefore, the site of localization of the fluorinated porphyrin **4** and the related chlorin **30** and bacteriochlorin **31** were compared with Rhodamine-123, which is known to target mitochondria. Images of the

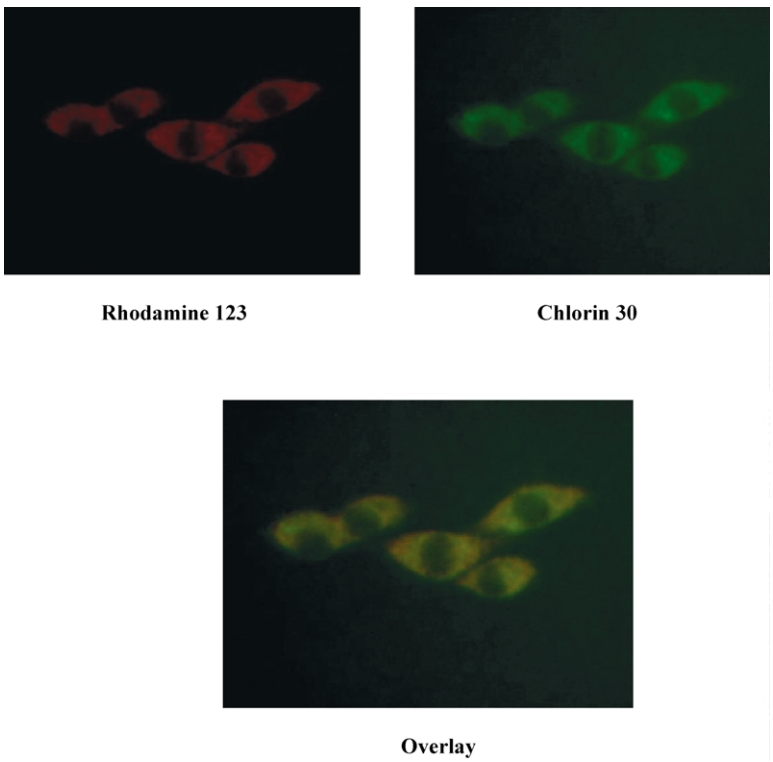

Figure 11. Comparative intracellular localization of Rhodamine-123 (mitochondrial probe) and fluorinated chlorin **30** in RIF cells at 24 h post-incubation. Similar patterns were observed from fluorinated porphyrin **4** and the corresponding bacteriochlorin **31** (only a representative example is shown). The overlay picture clearly indicates that both Rhodamine-123 and chlorin **30** localize in mitochondria.

photosensitizers and Rhodamine-123 were taken in rapid succession. The resulting images clearly indicate that these photosensitizers localize to the same cellular region as Rhodamine-123, suggesting that these compounds localize in mitochondria, a more sensitive site for cell damage by PDT (see Figure 11 for a representative example).

3. Experimental

3.1. Chemistry

All chemicals were of reagent grade and used as received. Solvents were dried using standard methods unless stated otherwise. Reactions were carried out under a N_2 atmosphere and were monitored by analytical precoated (0.20 mm) silica TLC plates (POLYGRAM® SIL N-HR). Melting points were determined on electrically heated melting point apparatus and are uncorrected. UV–vis spectra were recorded on a Varian (Cary-50 Bio) spectrophotometer. ^{1}H and ^{19}F NMR spectra were recorded on a Brucker AMX 400 and 376.5 MHz NMR spectrometer, respectively at 303°K in $CDCl_3$ containing tetramethylsilane (TMS) as an internal standard. Proton chemical shifts (δ) are reported in parts per million (ppm) relative to TMS (0.00 ppm) or $CDCl_3$ (7.26 ppm) while fluorine chemical shifts are reported in ppm relative to trifluoroacetic acid (0.00 ppm). Coupling constants (J) are reported in Hertz (Hz) and s, d, t, q, m, dd and br refer to singlet, doublet, triplet, quartet, multiplet, doublet of doublet and broad respectively. Mass spectral data (FAB) were obtained from the University of Michigan, East Lansing, MI (the matrix is usually nitrobenzyl alcohol) and from the Biopolymer Facility of Basic Studies Center, Roswell Park Cancer Institute, Buffalo, NY. Elemental analysis data were obtained from Midwest Microlab, LLC, Indianapolis, IN.

3.2. General method for the synthesis of dipyrromethane 6, 7 and 8

Pyrrole **5** (10.0 g, 0.055 mol) and *p*-methoxy benzaldehyde (3.74 g, 0.0275 mol) were dissolved in ethanol (70 mL) and *p*-toluenesulfonic acid (200 mg) was added. The reaction mixture was refluxed for 2 h under nitrogen. Analytical TLC at frequent intervals was used to monitor the completion of the reaction. It was then cooled, the solid was filtered, the product was washed with cold water and dried under vacuum at room temperature. The desired pyrromethane **6** [3,9-diethyl-6-(*p*-methoxyphenyl)-4,8-dimethyl-2,10-diethoxycarbonyl dipyrromethane] was isolated as a white powder in 80% (21.2 g) yield.

3.2.1. 3,9-Diethyl-6-(*p*-methoxyphenyl)-4,8-dimethyl-2,10-diethoxycarbonyl dipyrromethane (6). Mp 105–108°C; ^{1}H NMR: δ 8.20 (brs, 2H, 2×NH), 7.01 (d, J=8.9 Hz, 2H, ArH), 6.87 (d, J=8.9 Hz, 2H, ArH), 5.43 (s, 1H, CH), 4.26 (q, J=7.3 Hz, 4H, 2×OCH_2CH$_3$), 3.81 (s, 3H, OCH$_3$), 2.74 (q, J=7.5 Hz, 4H, 2×CH_2CH$_3$), 1.78 (s, 6H, 2×CH$_3$), 1.31 (t, J=7.1 Hz, 6H, 2×OCH$_2$CH_3), 1.12 (t, J=7.7 Hz, 6H, 2×CH$_2$CH_3). Anal. calcd for $C_{28}H_{36}N_2O_4$: C, 69.98; H, 7.55; N, 5.83. Found: C, 70.15; H, 7.37; N, 5.93. By following a similar approach, pyrrole **5** was reacted with *m*-methoxy or 3, 5-dimethoxy benzaldehyde and the corresponding dipyrromethane **7** and **8** were synthesized.

3.2.2. 3,9-Diethyl-6-(*m*-methoxyphenyl)-4,8-dimethyl-2,10-diethoxycarbonyl dipyrromethane (7). Yield 70%; mp 122–125°C; ^{1}H NMR: δ 8.25 (brs, 2H, 2×NH), 7.23–7.27 (m, 1H, ArH), 6.82 (dd, J=2.2, 7.8 Hz, 1H, ArH), 6.68 (d, J=7.4 Hz, 1H, ArH), 6.63 (s, 1H, ArH), 5.45 (s, 1H, CH), 4.25 (q, J=7.3 Hz, 4H, 2×OCH_2CH$_3$), 3.76 (s, 3H, OCH$_3$), 2.73 (q, J=7.6 Hz, 4H, 2×CH_2CH$_3$), 1.79 (s, 6H, 2×CH$_3$), 1.30 (t, J=7.1 Hz, 6H, 2×OCH$_2$CH_3), 1.11 (t, J=7.3 Hz, 6H, 2×CH$_2$CH_3). Anal. calcd for $C_{28}H_{36}N_2O_5$: C, 69.98; H, 7.55; N, 5.83. Found: C, 70.08; H, 7.60; N, 5.82.

3.2.3. 3,9-Diethyl-6-(3′,5′-dimethoxyphenyl)4,8-dimethyl-2,10-diethoxycarbonyldipyrromethane (8). Yield 60%; viscous oil; ^{1}H NMR: δ 8.25 (brs, 2H, 2×NH), 6.38 (s, 1H, ArH), 6.24 (s, 2H, ArH), 5.39 (s, 1H, CH), 4.26 (q, J=7.3 Hz, 4H, 2×OCH_2CH$_3$), 3.74 (s, 6H, 2×OCH$_3$), 2.70–2.78 (m, 4H, 2×CH_2CH$_3$), 1.79 (s, 6H, 2×CH$_3$), 1.32 (t, J=7.2 Hz, 6H, 2×OCH$_2$CH_3), 1.10–1.16 (m, 6H, 2×CH$_2$CH_3).

3.3. General method for the preparation of pyrromethanes 9, 11, 13

The diethoxycarbonyl dipyrromethanes **6**, **7** or **8** (for example 11.6 g of **6**) were individually dissolved in ethylene glycol (250 mL). Sodium hydroxide (12 g, crushed powder) was added, and the reaction mixture was refluxed for 1 h. It was then cooled, diluted with dichloromethane (250 mL) and washed with water (2×200 mL). The dichloromethane layer was dried over anhydrous sodium sulfate. The residue obtained after evaporating the solvent was chromatographed over silica column eluted with chloroform. The appropriate eluates were combined, the solvent was evaporated, and the desired dipyrromethane **9** was obtained in 95% yield.

3.3.1. 3,9-Diethyl-6-(*p*-methoxyphenyl)4,8-dimethyl-dipyrromethane (9). Mp 64–66°C; lit.[21] ^{1}H NMR: δ 7.30 (brs, 2H, 2×NH), 7.06 (d, J=8.8 Hz, 2H, ArH), 6.85 (d, J=8.8 Hz, 2H, ArH), 6.38 (s, 2H, 2×Pyrrolic CH), 5.45 (s, 1H, CH), 3.81 (s, 3H, OCH$_3$), 2.44 (q, J=7.2 Hz, 4H, 2×CH_2CH$_3$), 1.81 (s, 6H, 2×CH$_3$), 1.19 (t, J=7.9 Hz, 6H, 2×CH$_2$CH_3).

3.3.2. 3,9-Diethyl-6-(*m*-methoxyphenyl)-4,8-dimethyl-dipyrromethane (11). Yield 88%; mp 202–204°C; ^{1}H NMR: δ 9.49 (s, 2H, 2×CHO), 9.08 (brs, 2H, 2×NH), 7.23–7.27 (m, 1H, ArH), 6.83 (dd, J=2.5, 8.0 Hz, 1H, ArH), 6.66 (d, J=7.6 Hz, 1H, ArH), 6.62 (s, 1H, ArH), 5.53 (s, 1H, CH), 3.75 (s, 3H, OCH$_3$), 2.71 (q, J=7.6 Hz, 4H, 2×CH_2CH$_3$), 1.86 (s, 6H, 2×CH$_3$), 1.20 (t, J=7.8 Hz, 6H, 2×CH$_2$CH_3). Anal. calcd for $C_{22}H_{28}N_2O.2H_2O$: C, 70.94; H, 8.66; N, 7.52. Found: C, 71.29; H, 7.17; N, 7.24.

3.3.3. 3,9-Diethyl-6-(3′,5′-dimethoxyphenyl)-4,8-dimethyl-dipyrromethane (13). Yield 97%; mp 119–121°C; ^{1}H NMR: δ 7.34 (brs, 2H, 2×NH), 6.33–6.36 (m, 3H, ArH), 6.31 (s, 2H, 2×pyrrolic CH), 5.40 (s, 1H, CH), 3.74 (s, 6H, 2×OCH$_3$), 2.40–2.45 (m, 4H, 2×CH_2CH$_3$), 1.81 (s, 6H,

2×CH_3), 1.14–1.19 (m, 6H, 2×CH_2CH_3). Anal. calcd for $C_{23}H_{30}N_2O_2.5H_2O$: C, 60.50; H, 8.83; N, 6.40. Found: C, 60.00; H, 8.82; N, 5.91.

3.4. General method for the preparation of diformyldipyrromethanes 10, 12 and 14

The pyrromethane(s) [e.g. **9** (7.1 g)] was dissolved in Vilsmeier reagent, prepared by reaction $POCl_3$ (10.5 mL) and DMF (45 mL) was added and the reaction mixture was stirred at room temperature overnight. The reaction mixture was poured into ice cold water (250 mL) and aqueous sodium hydroxide (50%, 35 mL) was then added slowly; the pH was adjusted to 10–12 and stirred overnight before extracting with dichloromethane (3×200 mL). The organic layer was separated, washed with water (2×200 mL) until neutral and dried over anhydrous sodium sulfate. Evaporation of the solvent gave a residue which was chromatographed over a silica column, eluting with 1:1 ethyl acetate/cyclohexane. The major band was separated, and the product obtained after evaporating the solvent was crystallized with methanol and compound **10** was isolated in 80% (6.80 g) yield.

3.4.1. 3,9-Diethyl-2,10-diformyl-6-(*p*-methoxyphenyl)-4,8-dimethyldipyrromethane (10). Mp 168–169°C; ^{1}H NMR: δ 9.50 (s, 2H, 2×CHO), 8.70 (brs, 2H, 2×NH), 6.98 (d, J=8.7 Hz, 2H, ArH), 6.86 (d, J=8.7 Hz, 2H, ArH), 5.47 (s, 1H, CH), 3.80 (s, 3H, OCH_3), 2.70 (q, J=7.5 Hz, 4H, 2×CH_2CH_3), 1.81 (s, 6H, 2×CH_3), 1.20 (t, J=7.5 Hz, 6H, 2×CH_2CH_3). Anal. calcd for $C_{24}H_{28}N_2O_3.1/2H_2O$: C, 71.80; H, 7.28; N, 6.98. Found: C, 71.69; H, 6.74; N, 6.76.

3.4.2. 3,9-Diethyl-2,10-diformyl-6-(*m*-methoxyphenyl)-4,8-dimethyldipyrromethane (12). Yield 79%; mp 202–204°C; ^{1}H NMR: δ 9.49 (s, 2H, 2×CHO), 9.08 (brs, 2H, 2×NH), 7.23–7.27 (m, 1H, ArH), 6.83 (dd, J=2.5, 8.0 Hz, 1H, ArH), 6.66 (d, J=7.6 Hz, 1H, ArH), 6.62 (s, 1H, ArH), 5.53 (s, 1H, CH), 3.75 (s, 3H, OCH_3), 2.71 (q, J=7.6 Hz, 4H, 2×CH_2CH_3), 1.86 (s, 6H, 2×CH_3), 1.20 (t, J=7.8 Hz, 6H, 2×CH_2CH_3). Anal. calcd for $C_{24}H_{28}N_2O_3$: C, 73.44; H, 7.19; N, 7.14. Found: C, 73.65; H, 7.29; N, 7.06.

3.4.3. 3,9-Diethyl-2,10-diformyl-6-(3,5-di-methoxyphenyl)-4,8-dimethyldipyrromethane (14). Yield 78%; mp 202–204°C; ^{1}H NMR ($CDCl_3$, 400 MHz) δ 9.52 (s, 2H, 2×CHO), 8.56 (brs, 2H, 2×NH), 6.40 (s, 1H, ArH), 6.20 (s, 2H, ArH), 5.42 (s, 1H, CH), 3.74 (s, 6H, 2×OCH_3), 2.70 (q, J=7.7 Hz, 4H, 2×CH_2CH_3), 1.81 (s, 6H, 2×CH_3), 1.20 (t, J=7.8 Hz, 6H, 2×CH_2CH_3). Anal. calcd for $C_{25}H_{30}N_2O_4.1/2H_2O$: C, 69.58; H, 7.24; N, 6.49. Found: C, 69.52; H, 7.00; N, 6.16.

3.5. General method for the synthesis of porphyrins 22–25

The diformyl dipyrromethane (e.g. **10**, 2.52 g, 6.43 mmol), and dipyrromethane **18** (2.04 g, 6.42 mmol) were dissolved in dichloromethane (500 mL). *p*-Toluenesulfonic acid (6.0 g) dissolved in methanol (100 mL) was added, and the reaction mixture was stirred at room temperature overnight under nitrogen atmosphere. A saturated solution of zinc acetate/methanol (125 mL) was added, and the reaction was stirred for another 12 h. It was then diluted with dichloromethane, washed with water and the organic layer was dried over anhydrous sodium sulfate. Evaporation of the solvent gave a residue which was dissolved in trifluoroacetic acid (30 mL) and stirred at room temperature for 30 min. The Zn-free porphyrin thus obtained after standard work-up was chromatographed over a short Grade III Alumina column and eluted with dichloromethane. The major band was collected and the solvent evaporated. The residue was crystallized from dichloromethane/hexane and porphyrin **22** was isolated in 17% (640 mg) yield.

3.5.1. 2,8,13,17-Tetraethyl-5-(*p*-methoxyphenyl)-3,7,12,18-tetramethylporphyrin (22). Mp 280–282°C; UV–vis [CH_2Cl_2, nm (ε, M^{-1} cm^{-1})] 403 (3.82×10^5), 503 (3.15×10^4), 535 (1.39×10^4), 571 (1.35×10^4), 623 (4.82×10^3); ^{1}H NMR: δ 10.13 (s, 2H, 2×*meso*H), 9.92 (s, 1H, *meso*H), 7.86 (d, J=9.0 Hz, 2H, ArH), 7.16 (d, J=9.0 Hz, 2H, ArH), 4.00–4.06 (m, 8H, 4×CH_2CH_3), 3.99 (s, 3H, OCH_3), 3.62 (s, 6H, 2×CH_3), 2.47 (s, 6H, 2×CH_3), 1.87 (t, J=7.7 Hz, 6H, 2×CH_2CH_3), 1.75 (t, J=7.6 Hz, 6H, 2×CH_2CH_3), −3.19 (brs, 1H, NH), −3.27 (brs, 1H, NH). Anal. calcd for $C_{39}H_{44}N_4O$: C, 80.10; H, 7.58; N, 9.58. Found: C, 80.14; H, 7.54; N, 9.62.

3.5.2. 2,8,13,17-Tetraethyl-5-(*m*-methoxyphenyl)-3,7,12,18-tetramethylporphyrin (23). Yield 30%; mp 270–272°C; ^{1}H NMR: δ10.16 (s, 2H, 2×*meso*H), 9.96 (s, 1H, *meso* H), 7.67 (d, J=7.2 Hz, 2H, ArH), 7.59 (t, J=7.8 Hz, 1H, ArH), 7.50 (s, 1H, ArH), 4.02–10 (m, 8H, 4×CH_2CH_3), 4.00 (s, 3H, OCH_3), 3.65 (s, 6H, 2×CH_3), 2.60 (s, 6H, 2×CH_3), 1.90 (t, J=7.7 Hz, 6H, 2×CH_2CH_3), 1.78 (t, J= 7.94 Hz, 6H, 2×CH_2CH_3), −3.20 (brs, 1H, NH), −3.35 (brs, 1H, NH). Anal. calcd for $C_{39}H_{44}N_4O$: C, 80.10; H, 7.58; N, 9.58. Found: C, 80.76; H, 7.60; N, 9.54.

3.5.3. 2,8-Diethyl-5-(3′,5′-dimethoxyphenyl)-2, 8-diethyl-13,17-bis-(2-methoxycarbonylethyl)-3,7,12,18-tetramethylporphyrin (25). The title compound was prepared by reacting diformyldipyrromethane **14** with dipyrromethane dicarboxylic acid **21** by following the procedure reported by Chen et al.[22]

3.6. General method for the synthesis of porphyrins 26–29

Reaction of porphyrins **22**–**25** (100 mg each) with ethereal boron tribromide solution afforded porphyrin **26**–**29** in 70–77%.

3.6.1. 2,8,13,17-Tetraethyl-5-(*p*-hydroxyphenyl)-3,7,12,18-tetramethylporphyrin (26). Yield 77%; mp >300°C; UV–vis [CH_2Cl_2, nm (ε, M^{-1} cm^{-1})] 404 (3.79×10^5), 503 (2.91×10^4), 536 (1.19×10^4), 570 (1.14×10^4); ^{1}H NMR: δ 10.15 (s, 2H, 2×*meso* H), 9.94 (s, 1H, *meso* H), 7.89 (d, J=9.2 Hz, 2H, ArH), 7.18 (d, J=8.7 Hz, 2H, ArH), 4.00–4.08 (m, 8H, 4×CH_2CH_3), 3.64 (s, 6H, 2×CH_3), 2.53 (s, 6H, 2×CH_3), 1.88 (t, J=7.7 Hz, 6H, 2×CH_2CH_3), 1.76 (t, J=7.5 Hz, 6H, 2×CH_2CH_3), −3.75 (brs, 2H, 2×NH). Anal. calcd for $C_{38}H_{42}N_4O$: C, 79.66; H, 7.42; N, 9.82. Found: C, 79.75; H, 7.45; N, 9.70.

3.6.2. 2,8,13,17-Tetraethyl-5-(*m*-hydroxyphenyl)-3,7,12,18-tetramethylporphyrin (27). Yield 72%; mp >300°C; UV–vis [CH_2Cl_2, nm (ε, M^{-1} cm^{-1})] 402 (5.00×10^5), 502 (4.03×10^4), 536 (1.76×10^4), 570 (1.61×10^4), 623 (4.60×10^3); ^{1}H NMR: δ 10.18 (s, 2H, 2×*meso* H), 9.98 (s, 1H, *meso*H), 7.69 (d, *J*=7.0 Hz, 2H, ArH), 7.61 (t, *J*=7.7 Hz, 1H, ArH), 7.51 (s, 1H, ArH), 4.04–4.12 (m, 8H, 4×CH_2CH$_3$), 3.66 (s, 6H, 2×CH$_3$), 2.58 (s, 6H, 2×CH$_3$), 1.91 (t, *J*=7.7 Hz, 6H, 2×CH$_2$CH_3), 1.79 (t, *J*=7.94 Hz, 6H, 2×CH$_2$CH_3), −3.85 to −3.75 (each brs, 1H, 2×NH). Anal. calcd for $C_{38}H_{42}N_4O$: C, 79.66; H, 7.42; N, 9.82. Found: C, 80.02; H, 7.37; N, 9.83.

3.6.3. 2,8,13,17-Tetraethyl-5-(3′,5′-di-hydroxyphenyl)-3,7,12,18-tetramethylporphyrin (28). Yield 75%; mp >300°C; UV–vis [CH_2Cl_2, nm (ε, M^{-1} cm^{-1})] 402 (4.16×10^5), 502 (3.45×10^4), 536 (1.62×10^4), 569 (1.49×10^4), 623 (6.50×10^3); ^{1}H NMR ($CDCl_3$, 400 MHz) δ 10.18 (s, 2H, 2×*meso*H), 9.98 (s, 1H, *meso* H), 7.05 (s, 2H, ArH), 6.69 (s, 1H, ArH), 4.04–4.12 (m, 8H, 4×CH_2CH$_3$), 3.66 (s, 6H, 2×CH$_3$), 2.67 (s, 6H, 2×CH$_3$), 1.90 (t, *J*=7.7 Hz, 6H, 2×CH$_2$CH_3), 1.80 (t, *J*=7.5 Hz, 6H, 2×CH$_2$CH_3). Anal. calcd for $C_{38}H_{42}N_4O_2.H_2O$: C, 75.47; H, 7.33; N, 9.26. Found: C, 75.31; H, 7.38; N, 9.14.

3.6.4. 2,8-Diethyl-5-(3′,5′-dimethoxyphenyl)-13,17-bis-(2-methoxycarbonylethyl)-3,7,12,18-tetramethylporphyrin (29). Yield 70%; mp >300°C; UV–vis [CH_2Cl_2, nm (ε, M^{-1} cm^{-1})] 403 (4.64×10^5), 502 (5.21×10^4), 536 (3.39×10^4), 571 (4.00×10^4); ^{1}H NMR: δ 10.18 (s, 2H, 2×*meso* H), 9.95 (s, 1H, *meso* H), 7.10 (s, 2H, ArH), 6.70 (s, 1H, ArH), 4.30–4.40 (m, 4H, 2×CH_2CH$_2$CO$_2$CH$_3$), 3.98–4.08 (m, 4H, 2×CH_2CH$_3$), 3.70 (s, 6H, 2×OCH$_3$), 3.65 (s, 6H, 2×CH$_3$), 3.30–3.40 (m, 4H, 2×CH$_2$CH_2CO$_2$CH$_3$), 2.66 (s, 6H, 2×CH$_3$), 1.80–1.90 (m, 6H, 2×CH$_2$CH_3). Anal. calcd for $C_{42}H_{46}N_4O_6.H_2O$: C, 63.69; H, 6.11; N, 7.08. Found: C, 63.32; H, 6.07; N, 6.41.

3.7. General method for the synthesis of porphyrins 1 to 4

3,5-Bis(trifluromethyl)benzylbromide (40 μL, 0.22 mmol) and anhydrous K_2CO_3 (250 mg) were added to a stirred solution of 5-(4-hydoxyphenyl)tetraethylporphyrin **26** (85 mg, 0.15 mmol) in dry acetonitrile (10 mL) and the reaction mixture was refluxed overnight under nitrogen. Solvent was evaporated under reduced pressure; water (20 mL) was poured and extracted with CH_2Cl_2 (2×20 mL). The combined organic extracts were washed with water (2×20 mL) and organic fraction was dried over Na_2SO_4. Removal of organic solvent in vacuo gave a crude solid residue, which was chromatographed over silica column using CH_2Cl_2 as an eluant to yield 77 mg (65%) of 5-[4-{3,5-Bis(trifluromethyl)benzyloxy}phenyl]tetraethylporphyrin **1** as purple plates.

3.7.1. 5-[4-{3,5-Bis(trifluromethyl)benzyloxy}phenyl]-2,8,13,17-tetraethyl-3,7,12,18-tetramethylporphyrin (1). Mp. 274–276°C; UV–vis [CH_2Cl_2, nm (ε, M^{-1} cm^{-1})] 403 (2.52×10^5), 502 (2.08×10^4), 535 (9.25×10^3), 570 (8.82×10^3), 624 (3.13×10^3); ^{1}H NMR: δ 10.21 (s, 2H, 2×*meso* C*H*), 10.00 (s, 1H, *meso* C*H*), 8.14 (s, 2H, Ar*H*), 7.98 (s, 1H, Ar*H*), 7.96 (d, *J*=4.5 Hz, 2H, Ar*H*), 7.31 (d, *J*=4.5 Hz, 2H, Ar*H*), 5.42 (s, 2H, OCH_2), 4.06–4.13 (m, 8H, 4×CH_2CH$_3$), 3.70 (s, 6H, 2×CH_3), 2.52 (s, 6H, 2×CH_3), 1.94 (t, *J*=7.7 Hz, 6H, 2×CH$_2$CH_3), 1.82 (t, *J*=7.5 Hz, 6H, 2×CH$_2$CH_3). ^{19}F NMR: δ 13.12 (s, 6F, 2×CF$_3$). Anal. calcd for $C_{47}H_{46}N_4F_6O.H_2O$: C, 69.27; H, 5.94; N, 6.87. Found: C, 69.37; H, 6.19; N, 6.33.

3.7.2. 5-[3-Bis{3,5-trifluromethyl)benzyloxy}phenyl]-2,8,13,17-tetraethyl-3,7,12,18-tetramethylporphyrin (2). Yield 96%; mp 109–110°C; UV–vis[CH_2Cl_2, nm (ε, M^{-1} cm^{-1})] 404 (9.49×10^4), 501 (6.83×10^3), 537 (4.27×10^3), 570 (4.98×10^3); ^{1}H NMR: δ 10.17 (s, 2H, 2×*meso* C*H*), 9.96 (s, 1H, *meso* C*H*), 7.94 (s, 2H, Ar*H*), 7.75–7.85 (m, 3H, Ar*H*), 7.62 (t, *J*=7.8 Hz, 1H, Ar*H*), 7.40 (dd, *J*=2.6, 7.8 Hz, 1H, Ar*H*), 5.32 (s, 2H, OCH_2), 4.00–4.10 (m, 8H, 4×CH_2CH$_3$), 3.65 (s, 6H, 2×CH_3), 2.53 (s, 6H, 2×CH_3), 1.89 (t, *J*=7.8 Hz, 6H, 2×CH$_2$CH_3), 1.77 (t, *J*=7.6 Hz, 6H, 2×CH$_2$CH_3), −3.10 and −3.30 (each brs, 1H, 2×NH). ^{19}F NMR: δ 13.00 (s, 6F, 2×CF$_3$). Mass (FAB) calcd for $C_{47}H_{46}N_4F_6O$: 796.35. Found: 797.36 (M+1).

3.7.3. 5-[3′,5′-Bis{3″,5″-trifluromethyl)benzyloxy}phenyl]-2,8,13,17-tetraethyl-3,7,12,18-tetra-methyl porphyrin (3). Yield 45%; mp 214–216°C; UV–vis[CH_2Cl_2, nm (ε, M^{-1} cm^{-1})] 403 (2.29×10^5), 502 (1.93×10^4), 536 (9.27×10^3), 570 (8.53×10^3), 623 (3.34×10^3); ^{1}H NMR: δ 10.20 (s, 2H, 2×*meso* C*H*), 9.98 (s, 1H, *meso* C*H*), 7.96 (s, 4H, Ar*H*), 7.87 (s, 2H, Ar*H*), 7.42 (d, *J*=2.9 Hz, 2H, Ar*H*), 7.12–7.16 (m, 1H, Ar*H*), 5.37 (s, 4H, 2×OCH_2), 4.03–4.10 (m, 8H, 4×CH_2CH$_3$), 3.66 (s, 6H, 2×CH_3), 2.60 (s, 6H, 2×CH_3), 1.91 (t, *J*=7.5 Hz, 6H, 2×CH$_2$CH_3), 1.78 (t, *J*=7.5 Hz, 6H, 2×CH$_2$CH_3). ^{19}F NMR: δ 12.98 (s, 12F, 4×CF$_3$). Anal. calcd for $C_{56}H_{50}N_4F_{12}O_2$: C, 64.74; H, 4.85; N, 5.39. Found: C, 64.20; H, 4.94; N, 5.00.

3.7.4. 5-[3′,5′-Bis{3″,5″-trifluromethyl)benzyloxy}phenyl]-2,8-diethyl-13,17-bis(2-methoxycarbonylethyl)-3,7-dimethylporphyrin (4). Yield 75%; mp 72–75°C; UV–vis [CH_2Cl_2, nm (ε, M^{-1} cm^{-1})] 404 (3.81×10^5), 502 (3.02×10^4), 536 (1.41×10^4), 570 (1.32×10^4), 624 (4.82×10^3), 653 (2.59×10^3); ^{1}H NMR: δ 10.16 (s, 2H, 2×*meso* C*H*), 9.97 (s, 1H, *meso* C*H*), 7.92 (s, 3H, Ar*H*), 7.81–7.84 (m, 3H, Ar*H*), 7.37 (d, *J*=2.0 Hz, 2H, Ar*H*), 7.11 (d, *J*=2.4 Hz, 1H, Ar*H*), 5.35 (s, 4H, 2×OCH_2), 4.40 (t, *J*=7.6 Hz, 4H, 2×CH_2CH$_2$CO$_2$CH$_3$), 4.00 (q, *J*=7.8 Hz, 4H, 2×CH_2CH$_3$), 3.67 (s, 6H, 2×OCH$_3$), 3.66 (s, 6H, 2×CH_3), 3.30 (t, *J*=7.6 Hz, 4H, 2×CH$_2$CH_2CO$_2$CH$_3$), 2.56 (s, 6H, 2×CH_3), 1.74 (t, *J*=7.4 Hz, 6H, 2×CH$_2$CH_3), −3.27 (brs, 1H, NH), −3.33 (brs, 1H, NH). ^{19}F NMR: δ 12.96 (s,12F, 4×CF$_3$). Anal. calcd for $C_{60}H_{54}N_4F_{12}O_6.H_20$: C, 61.43; H, 4.81; N, 4.77. Found: C, 61.56; H, 4.71; N, 4.71.

3.7.5. 5-{3′,5′-Bis(3″,5″-dimethylbenzyloxy)}phenyl-2,8-diethyl-13,17-bis(2-methoxycarbonylethyl)-3,7-dimethylporphyrin (4a). Yield 30%; mp 158–160°C; UV–vis [CH_2Cl_2, nm (ε, M^{-1} cm^{-1})] 404 (3.81×10^5), 502 (3.43×10^4), 536 (1.56×10^4), 570 (1.50×10^4), 623 (5.19×10^3); ^{1}H NMR ($CDCl_3$, 400 MHz) δ 10.18 (s, 2H, 2×*meso* C*H*), 9.98 (s, 1H, *meso* C*H*), 7.31–7.32 (m, 2H, ArH), 7.11 (brs, 1H, Ar*H*), 7.08 (s, 3H, Ar*H*), 6.99 (s, 1H, Ar*H*), 6.96 (brs, 2H, Ar*H*), 5.17 (s, 4H, 2×OCH_2), 4.42 (t, *J*=7.6 Hz, 4H, 2×CH_2CH$_2$CO$_2$CH$_3$), 4.04 (q, *J*=7.0 Hz, 4H, 2×CH_2CH$_3$), 3.70 (s, 6H, 2×OCH$_3$), 3.69 (s, 6H, 2×CH_3), 3.32 (t, *J*=7.8 Hz, 4H, 2×CH$_2$CH_2CO$_2$CH$_3$), 2.58 (s, 6H, 2×CH_3), 2.30

(s, 12H, 4×PhCH_3), 1.78 (t, J=7.4 Hz, 6H, 2×CH_2CH_3), −3.25 (brs, 1H, NH), −3.28 (brs, 1H, NH). Mass (FAB) Calcd for $C_{60}H_{66}N_4O_6$: 938.22. Found: 939.20 (M+1).

3.8. Synthesis of chlorin 30 and bacteriochlorin 31 from porphyrin 4

OsO_4 (75 mg) dissolved in diethyl ether (5 mL) was added to a stirred solution of **4** (100 mg) in dry CH_2Cl_2 (20 mL) and pyridine (0.2 mL). The reaction mixture was stirred at room temperature for 6 h. UV–vis spectrum showed two peaks at 645 nm (chlorin **30**, major, R_f=0.6 in 5% MeOH in CH_2Cl_2) and at 713 nm (bacteriochlorin **31**, minor, R_f=0.4 in 5% MeOH in CH_2Cl_2). The reaction was worked up by passing a stream of H_2S gas for one minute, diluted with CH_2Cl_2 (50 mL) and then filtered through fluted filter paper. The residue was washed with CH_2Cl_2 (3×50 mL), dried over Na_2SO_4. The solvent was concentrated and the crude mixture so obtained was purified by preparative TLC using 5% MeOH in CH_2Cl_2 as an eluant. Three bands were isolated. The fast moving band (10 mg) was identified as unreacted starting material **4**, the middle band (25 mg, 40%) was found to be chlorin **30** and the slowest moving band isolated in 13 mg (20%) was characterized as bacteriochlorin **31**.

3.8.1. 5-[3,5-Bis{3,5-bis(trifluromethyl)benzyloxy}phenyl]-2,8-diethyl-7,8-dihydroxy-3,7,12,18-tetramethyl-13,17-bis(2-methoxycarbonylethyl)porphyrin (30). Mp 172–174°C; UV–vis [CH_2Cl_2, nm (ε, M^{-1} cm^{-1})] 397 (4.44×10^5), 500 (4.16×10^4), 648 (1.17×10^5); ^{1}H NMR: δ 9.88 (s, 1H, *meso* C*H*), 9.61 (s, 1H, *meso* C*H*), 9.21 (s, 1H, *meso* C*H*), 7.97 (s, 2H, ArH), 7.91 (s, 2H, ArH), 7.88 (s, 1H, ArH), 7.84 (s, 1H, Ar*H*), 7.35 (s, 1H, Ar*H*), 7.12 (s, 1H, Ar*H*), 7.06 (s, 1H, Ar*H*), 5.40 (s, 2H, OCH_2), 5.30 (s, 2H, OCH_2), 4.24 (t, J=7.2 Hz, 2H, CH_2CH$_2$CO$_2$CH$_3$), 4.15 (t, J=7.4 Hz, 2H, CH_2CH$_2$CO$_2$CH$_3$), 3.96 (q, J=7.4 Hz, 2H, CH_2CH$_3$), 3.69 (s, 3H, OCH$_3$), 3.67 (s, 3H, OCH_3), 3.47 (s, 3H, CH_3), 3.44 (s, 3H, CH_3), 3.17 (t, J=7.6 Hz, 4H, 2×CH$_2$CH_2CO$_2$CH$_3$), 2.26 (s, 3H, CH_3), 2.23–2.34 (m, 3H, CH_3), 1.70 (t, J=7.8 Hz, 3H, CH_3), 0.89–0.93 (m, 2H, CH_2CH$_3$), 0.44 (t, J=8.0 Hz, 3H, CH$_2$CH_3), −2.32 (brs, 1H, NH), ^{19}F NMR: δ 12.98 (s, 6F, 2×CF_3), 12.99 (s, 6F, 2×CF_3). Mass (FAB) calcd. for $C_{60}H_{56}N_4F_{12}O_8$: 1188.12. Found: 1189.50 (M+1).

3.8.2. 5-[3,5-Bis{3,5-bis(trifluromethyl)benzyloxy}phenyl]-2,8-diethyl-7,8,17,18-tetrahydroxy-3,7,12,18-tetramethyl-13,17-bis(2-methoxycarbonylethyl)porphyrin (31). Mp 100–103°C; UV–vis (CH_2Cl_2) 395 (1.69×10^5), 504 (2.22×10^4), 644 (3.81×10^4), 716 (2.67×10^4). Note: Due to mixture of isomers it was difficult to assign the resonances for each proton in the ^{1}H NMR spectrum. The ^{19}F NMR spectrum showed mainly two peaks at δ 12.97 and 12.96 ppm. Mass (FAB) calcd for $C_{60}H_{58}N_4F_{12}O_{10}$: 1223.13. Found: 1223.30 (M+1).

3.9. Method for in vitro biological studies

The in vitro photosensitizing activity of fluorinated photosensitizers **1**–**4**, chlorin **30** and bacteriochlorin **31** was determined in the radiation induced fibrosarcoma (RIF) tumor cell line.[18] The RIF tumor cells were grown in α-MEM with 10% fetal calf serum, penicillin and streptomycin. Cells were maintained in 5% CO_2, 95% air and 100% humidity. For determining the PDT efficacy, these cells were plated in 96-well plates at a density of 1.25×10^4 cells well in complete media. After an overnight incubation at 37°C, the photosensitizers were added at the same concentration (1.0 μM), incubated at 37°C for 4 h in the dark. Cells were then illuminated with a 1000 W quartz halogen lamp with IR and band pass dichroic filters to allow light between 400 and 700 nm, at a dose rate of 16 mW/cm^2. After PDT, the cells were washed once and placed in complete media and incubated for 48 h. Then 10 μL of 5.0 mg/mL solution of 3-[4,5-dimethylthiazol-2-yl]-2,5-diphenyltetrazoliumbromide dissolved in PBS (Sigma, St. Louis, MO) was added to each well. After a 4 h incubation at 37°C the MTT and media were removed and 100 mL DMSO was added to solubilize the formazin crystals. The 96-well plate was read on a microtiter plate reader (Miles Inc. Titertek Multiscan Plus MK II) at 560 nm. The results were plotted as percent survival of the corresponding dark (drug no light) control for each compound tested. Each data point is the average of 5 replicate wells and the error bars are the standard deviation of a single experiment.

3.10. Intracellular localization

In order to determine the subcellular localization of the fluorinated porhyrin **4**, chlorin **30** and bacteriochlorin **31**, the RIF cells were seeded on poly-L-lysine coated glass cover slips at 1×10^5 in 6 well plates and cultered for 48 h to allow for attachment and spreading. The cells were incubated at 37°C in dark with the 1 μM concentration of photosensitizers for 1, 4 and 24 h and then co-incubated with the 0.25 μM concentration of the organelle-specific dyes Rhodamine-123 for mitochondria and Fluospheres for lysosomes. Immediately prior to microscopy (Zeiss Axiovert 35, Carl Zeiss, Inc. Germany), the cells were gently rinsed with PBS. Cells were illuminated with a mercury arc lamp with a filter cube containing 530–585 nm excitation filter, a 600 nm dichoric filter and a long pass emission filter to detect the photosensitizer. Fluorescent images were recorded and analyzed using a GenIISys intesifier coupled toa Dage MTI CCD72 camera and digitally processed with Metamorph software (Universal Imaging Corp., Downingtown, PA).

3.11. Photophysical measurements

Absorption spectra were recorded on a Hewlett Packard 8453A diode array spectrophotometer. Time-resolved fluorescence and phosphorescence spectra were measured by a Photon Technology International GL-3300 with a Photon Technology International GL-302, nitrogen laser/pumped dye laser system, equipped with a four channel digital delay/pulse generator (Stanford Research System Inc. DG535) and a motor driver (Photon Technology International MD-5020). Excitation wavelengths were from 535 to 551 nm using coumarin 540A (Photon Technology International, Canada) as a dye. Fluorescence lifetimes were determined by a two-exponential curve fit using a microcomputer. Nanosecond transient absorption measurements were carried out using a Nd:YAG laser (continuum, SLII-10, 4–6 ns fwhm) at 355 nm with the

power of 10 mJ as an excitation source. Photoinduced events were estimated by using a continuous Xe-lamp (150 W) and an InGaAs-PIN photodiode (Hamamatsu 2949) as a probe light and a detector, respectively. The output from the photodiodes and a photomultiplier tube was recorded with a digitizing oscilloscope (Tektronix, TDS3032, 300 MHz). The transient spectra were recorded using fresh solutions in each laser excitation. All experiments were performed at 298 K.

For the $^1O_2$ phosphorescence measurements, an O_2-saturated C_6D_6 solution containing the sample in a quartz cell (optical path length 10 mm) was excited at 532 nm using a Cosmo System LVU-200S spectrometer. A photomultiplier (Hamamatsu Photonics, R5509-72) was used to detect emission in the near infrared region (band path 1 mm).

3.12. Electrochemical and spectroelectrochemical measurements

Cyclic voltammetry (CV) measurements were performed at 298 K on an EG&G Model 173 potentiostat coupled with an EG&G Model 175 universal programmer in deaerated benzonitrile solution containing 0.1 M TBAP as a supporting electrolyte. A three-electrode system was utilized and consisted of a glassy carbon working electrode, a platinum wire counter electrode and a saturated calomel reference electrode (SCE). The reference electrode was separated from the bulk of the solution by a fritted-glass bridge filled with the solvent/supporting electrolyte mixture. Thin-layer spectroelectrochemical measurements of the one-electron oxidized and one-electron reduced bacteriochlorin derivatives were carried out using an optically transparent platinum thin-layer working electrode and a Hewlett–Packard model 8453 diode array spectrophotometer coupled with an EG&G Model 173 universal programmer.

3.13. In vivo ^{19}F measurements

The radiation induced fibrosarcoma (RIF) cells were maintained according to the protocol of Twentyman et al.[23] Tumors were grown on mouse foot dorsum by inoculating 2×10^5 cells. The photosensitizer was administered IP ($\sim$100 μM). ^{19}F MR spectra were collected on a Bruker 7T instrument using a home built surface coil. The ^{19}F MR spectral parameters included a 90° pulse of 16 μs, a spectral width of 20 KHz, 8 K data points, and a 2 s repetition time for a total accumulation time of 30 min.

Acknowledgements

This research was supported by grants from DOD (DMAD17-99-1-9065), NIH (CA 55792), the Robert A. Welch Foundation (Grant E-680 to KMK), from the Ministry of Education, Culture, Sports, Science and Technology, Japan (13440216 and 13031059 to SF) and the shared resources of the Roswell Park Cancer Center Support Grant (P30CA16056). We thank Beverly Chamberlin, Michigan State University, East Lansing for mass spectrometry results. The elemental analyses were performed at Midwest Micro lab, Indianapolis.

References

1. (a) Pandey, R. K.; Zheng, G. In *The Porphyrin Handbook*; Smith, K. M., Kadish, K. M., Guilard, R., Eds.; Academic: San Diego, 2000. (b) Dougherty, T. J.; Gomer, C.; Henderson, B. W.; Jori, G.; Kessel, D.; Kobrelik, M. J.; Peng, Q. *J. Natl. Cancer Inst.* **1998**, *90*, 889. (c) Bonnett, R. *J. Heterocycl. Chem.* **2002**, *39*, 455. (d) Boyle, R. W.; Rousseau, J.; Kudrevich, S. V.; Obochi, M. O. K.; van Lier, J. E. *Br. J. Cancer* **1996**, *73*, 49.
2. Sherman, W. M.; Allen, C. M.; van Lier, J. E. *Methods Enzymol.* **2000**, *319*, 376.
3. (a) Workman, P.; Maxwell, R. J.; Griffiths, J. R. *NMR Biomed.* **1992**, *5*, 270. (b) Blackstock, A. W.; Lightfoot, H.; Case, L. D.; Tepper, J. E.; Mukherji, S. K.; Mitchell, B. S.; Swarts, S. G.; Hess, S. M. *Clin. Cancer Res.* **2001**, *7*, 3263–3268. (c) Martino, R.; Malet-Martino, M.; Gilard, V. *Curr. Drug Metab.* **2000**, *1*, 271–303. (d) Hunjan, S.; Zhao, D.; Constantinescu, A.; Hahn, E. W.; Antich, P. P.; Mason, R. P. *Int. J. Radiat. Oncol. Biol. Phys.* **2001**, *49*, 1097–1108.
4. Bottomly, P. A. *Radiology* **1989**, *170*, 1.
5. Mason, R. P.; Shukla, H.; Antich, P. P. *Magn. Reson. Med.* **1993**, *29*, 296.
6. (a) Ceckler, T. L.; Gibson, S. L.; Hilf, R.; Bryant, R. G. *Magn. Reson. Med.* **1990**, *13*, 416. (b) Thomas, C.; Counsell, C.; Wood, P.; Adams, G. *Bull. Cancer* **1993**, *80*, 666.
7. Jameson, C. J. In *Fluorine*; Mason, J., Ed.; Plenum: New York, 1987; p 437 Chapter 16.
8. Omote, M.; Ando, A.; Takagi, T.; Koyama, M.; Kumadaki, I. *Tetrahedron* **1996**, *52*, 13961.
9. Barton, D. H. R.; Zard, S. Z. *J. Chem. Soc. Chem. Commun.* **1985**, 1098.
10. Caveleiro, J. A. S.; Gonsalves, J. A. S.; Kenner, A. M. d.'A. R.; Smith, G. W. K. M. *J. Chem. Soc. Perkin Trans.* **1973**, 240.
11. Jackson, A. H.; Smith, K. M. *The Total Synthesis of Natural Products*; ApSimon, J., Ed.; Wiley: New York, 1973; Vol. 3, p 144 1984, Vol. *6*, p 23.
12. Arsenault, G. P.; Bullock, E.; MacDonald, S. F. *J. Am. Chem. Soc.* **1960**, *82*, 4384.
13. Clezy, P. S.; Fookes, C. J. R.; Liepa, A. J. *Aust. J. Chem.* **1977**, *30*, 2017.
14. (a) Pandey, R. K.; Jackson, A. H.; Smith, K. M. *J. Chem. Soc. Perkin Trans. 1* **1991**, 1211. (b) Smith, K. M.; Pandey, R. K. *Tetrahedron Lett.* **1986**, *27*, 2717. (c) Jackson, A. H.; Pandey, R. K.; Rao, K. R. N.; Roberts, E. *Tetrahedron Lett.* **1985**, 793.
15. Smith, K. M. In *The Porphyrins and Metalloporphyrins*; Smith, K. M., Ed.; Elesvier: Amsterdam, 1975.
16. Fukuzumi, S.; Suenobu, T.; Patz, M.; Hirasaka, T.; Itoh, S.; Fujitsuka, M.; Ito, O. *J. Am. Chem. Soc.* **1998**, *120*, 8060.
17. Arbogast, J. W.; Darmanyan, A. P.; Chrostopher, P. D.; Foote, S.; Rubin, Y.; Diederich, F. N.; Alvarez, M. M.; Anz, S. J.; Whetten, R. L. *J. Phys. Chem.* **1991**, *95*, 11.
18. Felton, R. H. *The Porphyrins*; Dolphin, D., Ed.; Academic: New York, 1978; Vol. 5. Chapter 3.
19. (a) Pandey, R. K.; Sumlin, A. B.; Potter, W. R.; Bellnier, D. A.; Henderson, B. W.; Constantine, S.; Aoudia, M.; Rodgers, M. A. J.; Smith, K. M.; Dougherty, T. J. *Photochem. Photobiol.* **1996**, *63*, 194. (b) Henderson, B. W.; Bellnier, D. A.; Graco, W. R.; Sharma, A.; Pandey, R. K.; Vaughan, L.; Weishaupt, K. R.; Dougherty, T. *J. Cancer Res.* **1997**, *57*, 4000. (c) Zheng, G.; Potter, W. R.; Camacho, S. H.; Missert, J. R. G.; Wang, G.; Bellnier, D. A.; Henderson, B. W.;

Rodgers, M. A. J.; Dougherty, T. J.; Pandey, R. K. *J. Med. Chem.* **2001**, *44*, 1540. and references therein.
20. Pandey, R. K.; Potter, W. R.; Meunier, I.; Sumlin, A. B.; Smith, K. M. *Photochem. Photobiol.* **1995**, *62*, 764.
21. Li, G.; Graham, A.; Potter, W. R.; Grossman, Z. D.; Oseroff, A.; Dougherty, T. J.; Pandey, R. K. *J. Org. Chem.* **2001**, *66*, 1316.
22. Chen, Y. C.; Medforth, C. J.; Smith, K. M.; Alderfer, J. L.; Dougherty, T. J.; Smith, K. M. *J. Org. Chem.* **2001**, *66*, 3930.
23. Twentyman, P. R.; Brown, J. M.; Gray, J. W.; Franko, A. J.; Scoles, M. A.; Kallman, R. F. *J. Natl. Cancer Inst.* **1980**, *64*, 595.